Influence of Contact Solid Angle on Anode Spot Formation Threshold Current in Vacuum Circuit Breakers

Guowei Kong, Zhiyuan Liu, Yingsan Geng, Hui Ma, Xiaohui Xue
State Key Laboratory of Electrical Insulation and Power Equipment,
Xi'an Jiaotong University, Xi'an, China

Abstract- **The objective of this paper is to experimentally understand a relationship between anode spot formation threshold current I_{th} and a contact solid angle in vacuum arcs subjected to an axial magnetic field (AMF). Experiments were performed in a demountable vacuum chamber, in which an axial magnetic field coil was installed coaxially with a pair of butt contacts. Solid angle Ω is subtended by the anode of the cathode center In the experiment, butt type contacts with contact material CuCr25 and contact diameter 12 mm, 25 mm, 40mm, 60mm and 80 mm were tested. At the end of arcing, the contact separation was about 12~24 mm determined by an opening velocity with arcing time about 10 ms. The AMF applied to the pair of butt type contact was adjusted from 0 to 122 mT. Arc current was tested up to 30 kA at 50 Hz. The results showed that anode spot formation threshold current I_{th} was linearly proportional to not only contact solid angle but also the AMF applied. Besides, the influence of contact separation length on I_{th} was not as significant as that of contact diameter. With increasing of AMF, the anode surface temperature at current zero in the condition of I_{th} declined and also the temperature distribution tended to shrink.**

I. INTRODUCTION

A successful high-current interruption in vacuum is severely influenced by anode phenomena of the vacuum arc. When the arc current exceeds a threshold level I_{th}, an anode spot comes to form suddenly. High-current anode spot phenomenon causes gross electrodes erosion or even mass metal vapor after current zero often followed by a failure of interruption [1].

There are many influence parameters for anode spot formation, such as contact material, contact diameter, contact separation and magnetic fields, etc [2, 3]. It is proved that anode spot formation threshold current is closely related to contact diameter and contact separation [3-7].The threshold current I_{th} increases with anode diameter and decreases with contact separation. Mitchell [4] pointed out a starvation current correlated to anode spot formation was inversely proportional to contact separation. And the starvation current was proportional to the anode diameter to the power of 1.2. Similar results were found in the other research [5-7].

Compared with anode diameter or contact separation alone, contact solid angle was often a more important geometrical parameter to investigate the anode spot formation threshold current I_{th} [3]. As shown in Fig. 1, contact solid angle Ω is subtended by the anode of the cathode center. The interactions between anode spot formation threshold current I_{th} and contact solid angle have been evidenced by the results in the past work [8-10]. The results revealed that I_{th} could increase with contact solid angle [8-10].

Besides, as well known that the anode spot threshold current I_{th} is well influenced by an axial magnetic field (AMF) flux density in the vacuum arc [11, 12]. AMF contributed to improve threshold current level of anode spot formation significantly [13]. With an AMF applied, positive ion in vacuum arc plasma was prevented escaping from contact gap. This effect caused decrease of arc voltage and increase of arc current density on anode surface, which resulted in improvement of anode spot threshold current [11-13].

Generally, although the relationship between vacuum arc anode spot formation threshold current I_{th} and contact solid angle has been evidenced, but the results in the past work were scattered and there lacked of a systematic research on anode spot formation threshold current influenced by contact solid angle and AMF in combination at a unified experimental condition. The objective of this paper is to experimentally understand the relationship between anode spot formation threshold current and the contact solid angle in vacuum arcs subjected to axial magnetic fields. The results may provide more experimental evidence for anode spot formation theory and for development of high-capacity vacuum interrupters.

II. EXPERIMENTAL SETUP

The experiments were done in a demountable vacuum chamber which was evacuated to 10^{-3}~10^{-4} Pa. The experimental setup is shown in Fig. 1. Through an observing windows located on the chamber, a high-speed charge-coupled device (CCD) video camera was used to record the vacuum arc evolution and a two-color pyrometer was used to record temperature on the anode surface at current zero. The camera recording speed was set to be 10000 frames/s with the aperture fixed at 4 and the exposure time was set as 2 μs. The temperature measurement range of the two-color pyrometer was from 1073K to 1873K.

This work was supported by the National Natural Science Foundation of China under Project No. 51177122 and by the State Key Laboratory of Electrical Insulation and Power Equipment Fund under Grant EIPE11118.

978-1-4673-1265-3/12/$31.00 ©2012 IEEE

To generate a uniform axial magnetic field (AMF), an external Helmholtz coil passing through a direct current from a DC current source was installed coaxially with the pair of contacts in the chamber. The 80 turns Helmholtz coils had an average radius and center to center separation of 16 cm. The current source ranged up to 400 A was turned on about 100 ms before arcing. And the AMF flux density applied was at the range of 0 ~ 122 mT with the direction controlled from the up contact to the down contact in the chamber.

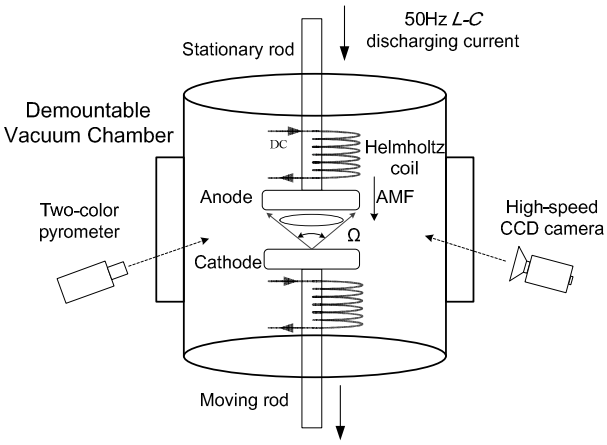

Fig. 1. Experimental setup for the research.

Experiments were performed in a L−C discharging circuit with current frequency 50 Hz and the arc currents used were up to 30 kArms. As shown in Fig. 2(a), the movable cathode in each experiment was controlled electronically to separate at the third half-wave 50 Hz current. The arcing time was sustained about 10 ms.

Contact solid angle Ω is subtended by the anode of the cathode center or by a ratio of the anode diameter to the contact distance. Fig. 2(b) shows two different types of solid angle. Ω_1 is subtended by the ratio of the anode diameter to contact separation length at arc extinguish (D/l). While Ω_2 is subtended by the anode diameter to contact gap (D/g). Since the vacuum arc evolution performs to be a dynamic process during arcing, it is more meaningful for Ω_1 to study high-current anode phenomena in vacuum arc than Ω_2. So the ratio of the anode diameter to the contact separation at arc extinguish D/l in the experiments was used as the contact solid angle for the research of high-current anode spot phenomena in vacuum.

Butt type contacts with thickness 5 mm were used in the experiment. And the contact material was CuCr25 with contact diameter 12 mm, 25 mm, 40 mm, 60 mm and 80 mm, respectively. The contact separation lengths were adjusted by the average opening velocity within the arcing time about 10 ms. The average opening velocity was defined as an average velocity within the contact separation during arcing time, which was set as about 1.2 m/s, 1.8 m/s and 2.4 m/s, respectively. Thus contact separation length l at arc extinguish was adjusted to about 12 mm, 18 mm and 24 mm, respectively. In the experiment, the contact gap was set as 38 mm.

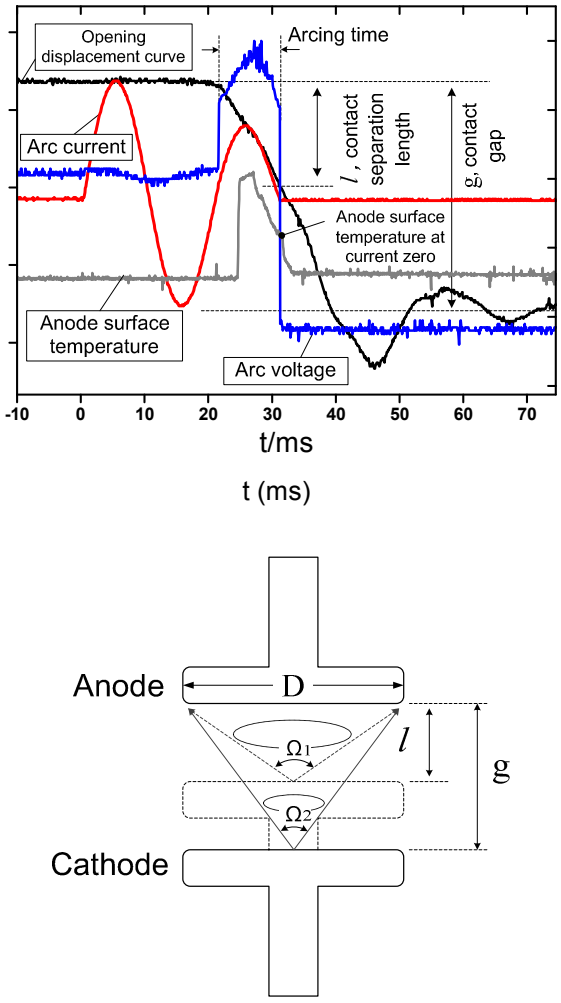

(b)

Fig. 2. Experimental parameters for high-current anode spot phenomena observation. (a) Waveform of arc current, arc voltage, and displacement curve; (b) Definition of contact solid angle.

III. EXPERIMENT RESULT

A. High-current vacuum arc anode phenomena

As Miller [2] pointed out a vacuum arc can exhibit three high-current anode discharge modes including a footpoint mode, an anode spot mode and an intense arc mode. A footpoint was much cooler than a true anode spot and usually evolved instantaneously to an anode spot in a vacuum arc.

In the experiment, both the footpoint mode and the anode spot mode were classified to a high-current anode spot mode. Here the high-current anode spot discharge mode was defined by the characteristics: There is a luminous or bright region on the anode; arc voltage noise tends to be higher; arc plasma concentrates around the anode surface or even with arc jet in both contacts; anode erosion is obvious [2, 14]. The typical anode spot photos in the experiment are shown in Fig. 3.

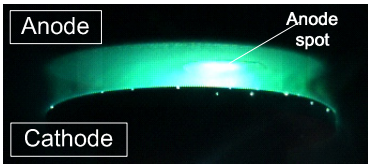

(a)

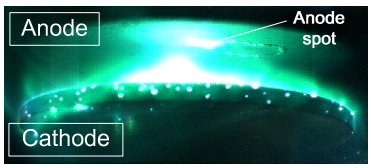

(b)

Fig. 3. Typical anode spot discharge mode photos. Contact material CuCr25, contact diameter 60mm, AMF 37mT. (a) *l* ~12mm,14.4kA; (b) *l* ~24mm, 11.0kA.

B. *Anode spot formation threshold current I_{th}*

The relationship between anode spot formation threshold current I_{th} and contact solid angle *D*/*l* subjected to different AMF was investigated in the experiment. With the arcing time fixed at about 10ms, the contact solid angle *D*/*l* was both adjusted by the contact diameter *D* with the same contact separation length *l* and also adjusted by *l* with the same *D*.

Fig. 4 shows the characteristic of anode spot formation threshold current I_{th} as a function of contact solid angle *D*/*l* adjusted by contact diameter with a setting contact separation about 24 mm. The contact diameter *D* was 12 mm, 25 mm, 40 mm, 60 mm and 80 mm, respectively. Fig. 4 shows a linear relationship between I_{th} and *D*/*l* adjusted by contact diameter *D*. It also indicates that I_{th} increased with AMF when *D*/*l* was more than about 1.0 corresponding to *D* high than 25 mm. While at the *D*/*l* about 0.5 corresponding to *D* 12 mm, I_{th} was inversely proportional to AMF.

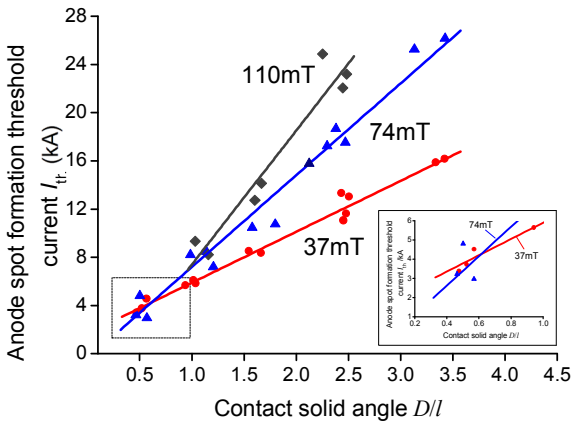

Fig. 4. Anode spot formation threshold current I_{th} and contact solid angle *D*/*l* adjusted by *D*. CuCr25, Arcing time ~10 ms, Average contact opening velocity 2.4 m/s, Contact diameter *D* 12 mm, 25 mm, 40 mm, 60 mm and 80 mm, respectively.

Fig. 5 shows the characteristic of anode spot formation threshold current I_{th} as a function of contact solid angle *D*/*l* adjusted by contact separation length *l* with a fixed contact diameter *D* 60 mm. The contact separation could be adjusted by average contact opening velocity with a arcing time about 10 ms. In the experiment, the average contact opening velocities were set as 1.2 m/s, 1.8 m/s and 2.4 m/s respectively. Thus the contact separation lengths *l* was about 12 mm, 18 mm and 24 mm, respectively. Fig. 5 also shows a linear relationship between I_{th} and *D*/*l* adjusted by contact separation length *l*. And I_{th} increased with AMF significantly.

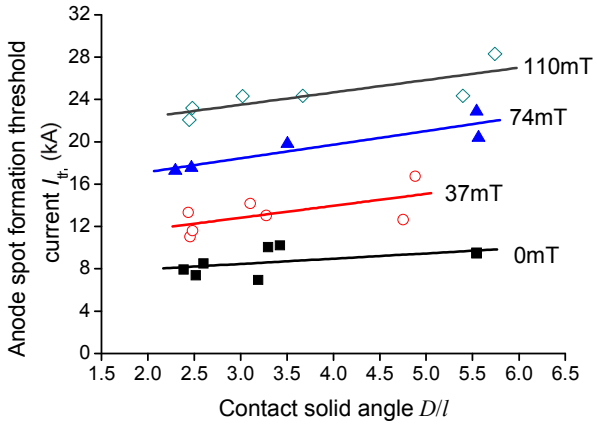

Fig. 5. Anode spot formation threshold current I_{th} and contact solid angle *D*/*l* adjusted by *l*. CuCr25, *D* 60mm, Arcing time ~10ms, Average contact opening velocities 1.2m/s, 1.8m/s and 2.4m/s, respectively.

And the relationship between anode spot formation threshold current I_{th} and AMF flux density was also investigated specially in the experiment. As shown in Fig. 6, the contact diameter *D* was 60mm with two contact solid angle *D*/*l* of about 2.5 and 3.5. The AMF flux density was 0 mT, 20 mT, 37 mT, 56 mT, 76 mT, 93 mT, 110 mT and 122 mT, respectively. Fig. 6 shows that the anode spot formation threshold current I_{th} was linearly proportional to AMF.

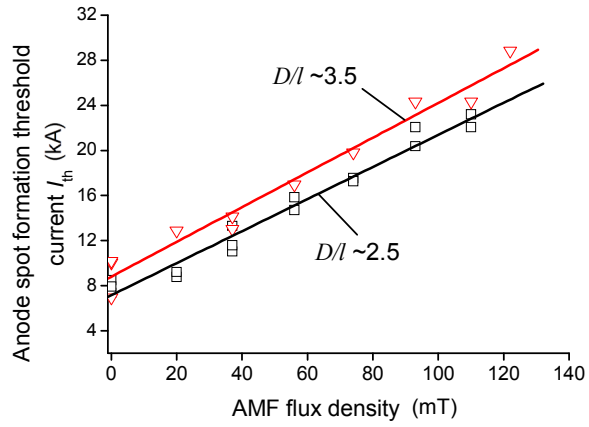

Fig. 6. Anode spot formation threshold current I_{th} and AMF flux density. CuCr25, *D* 60 mm, Arcing time ~10 ms, Average contact opening velocities, 1.8 m/s and 2.4 m/s, respectively.

C. *Anode spot temperature at current zero*

Fig. 7 shows the characteristics of anode surface temperature at current zero of the anode spot

formation threshold current I_{th} in the experiment. As shown in Fig. 7, although the threshold current I_{th} increased with an increasing AMF for a setting contact solid angle D/l, the anode surface temperature at current zero in the condition of I_{th} declined with increasing of AMF and also the temperature distribution tended to shrink. It also revealed that there was no obvious relationship between contact solid angle D/l and anode surface temperature at current zero in the condition of I_{th}. While in Fig. 7, since there was no light filter applied to the two-color pyrometer to avoid UV (UltraViolet) arc light. Some temperature values were recorded more than 1873 K which was set as a full range of the measure equipment.

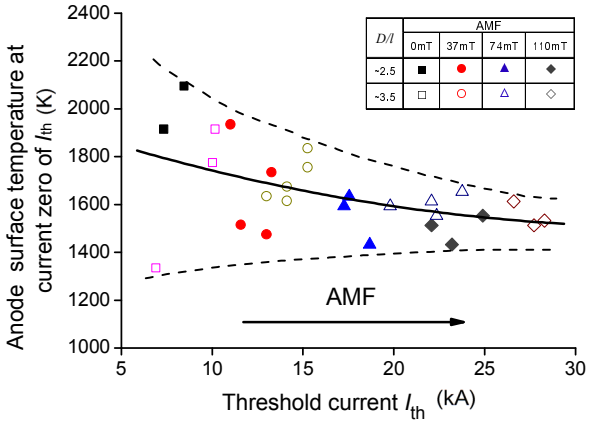

Fig. 7. The anode surface temperature at current zero of I_{th}. CuCr25, D 60 mm, Arcing time ~10 ms, Average contact opening velocities, 1.8 m/s and 2.4 m/s, respectively.

IV. DISCUSSION

From Fig. 4, it seems that the anode spot formation threshold current I_{th} decreased with AMF flux density at a small contact diameter 12mm. The result was quite different to a general acceptance. The phenomenon may be explained by the following: For a very small contact diameter, the constriction of arc current density on anode surface affected by AMF is so immense that the arc energy on anode is overloaded. That effect could result in a decrease of anode spot formation threshold current.

The results in Fig. 4 and Fig. 5 indicate that the influence of contact separation length l on anode spot formation threshold current I_{th} is not as significant as contact diameter D. The reason may be that the larger contact solid angle D/l when adjusted by l corresponds to smaller l. In that condition, vacuum arc is determined by an intense arc mode not by an anode spot mode.

V. CONCLUSION

In this paper, the influence of contact solid angle on anode spot formation threshold current in vacuum arcs subjected to axial magnetic fields has been studied. The conclusions are in the following:

1) The anode spot formation threshold current I_{th} was linearly proportional to contact solid angle D/l adjusted by contact diameter D or by contact separation length l. But the influence of l on I_{th} was not as significant as that of D.
2) I_{th} increased with AMF at different contact diameter D condition in the experiment except small D 12mm.
3) I_{th} was linearly proportional to AMF at D 60mm.
4) The anode surface temperature at current zero of I_{th} declined and also the temperature distribution tended to shrink, with increasing of AMF.

REFERENCES

[1] P. G. Slade, "The vacuum interrupter theory design and application," CRC Press, Boca Raton, 2008, pp. 294.

[2] H. C. Miller, "A Review of Anode Phenomena in Vacuum Arcs," *IEEE Trans. Plasma Sci.*, vol. 13, pp. 242-252, Oct. 1985.

[3] H. C. Miller, "Anode phenomena," in *Handbook of Vacuum Arc Science and Technology, Fundamentals and Applica- tions*, R. L. Boxman, P. J. Martin, and D. M. Sanders, Eds. Park Ridge, NJ: Noyes, 1995, pp 308-364.

[4] G. R. Mitchell, "High-current vacuum arcs. Part 1 An experimental study," *Proc. Inst. Electr. Eng.*, vol. 117, no. 12, pp. 2315–2326, Dec. 1970.

[5] K. Watanabe, E. Kaneko, and S. Yanabu, "Technological progress of axial magnetic field vacuum interrupters," *IEEE Trans. Plasma Sci.*, vol. 25, pp. 609-616, Aug. 1997.

[6] E. Schade, "Physics of high-current interruption of vacuum circuit breakers," *IEEE Trans. Plasma Sci.*, vol. 33, pp. 1564-1575, Oct. 2005.

[7] R. L. Boxman, J. H. Harris, and A. Bless, "Time-Dependence of Anode Spot Formation Threshold Current in Vacuum Arcs," *IEEE Trans. Plasma Sci.*, vol. 6, pp. 233-237, Sep. 1978.

[8] M. G. Drouet, "Current Distribution at anode and current flow in the interelectrode region of the vacuum arc," *in Proc. 12th Int. Symp. Discharges Elect. Insulation Vacuum*, Shoresh, Israel, 1986, pp. 120–124.

[9] D. L. Shmelev, "MHD model of plasma column of high current," *in Proc. 19th Int. Symp. Discharges Elect. Insulation Vacuum*, Xi'an, China, 2000, pp. 214–217.

[10] Z. Liu, S. Cheng, Y. Zheng, M. Rong, and J. Wang, "Comparison of Vacuum Arc Behaviors Between Axial-Magnetic-Field Contacts," *IEEE Trans. Plasma Sci.*, vol. 36, pp. 200-207, Feb. 2008.

[11] M. B. Schulman and J. A. Bindas, "Evaluation of Ac Axial Magnetic-Fields Needed to Prevent Anode Spots in Vacuum Arcs between Opening Contacts," *IEEE Trans. Compon. Packag. Technol. A*.*, vol. 17, pp. 53-57, Mar. 1994.

[12] C. W. Kimblin, "Arcing And Interruption Phenomena In Ac Vacuum Switchgear And In Dc Switches Subjected To Magnetic-Fields," *IEEE Trans. Plasma Sci.*, vol. 11, pp. 173-181, Sep. 1983.

[13] S. Yanabu, Y. Satoh, T. Tamagawa, E. Kaneko, and S. Sohma, "10 Years Experience In Axial Magnetic Field-Type Vacuum Interrupters," *IEEE Trans. Power Del.*,vol. 1, pp. 202-208, Oct. 1986.

[14] G. Kong, Z. Liu, D. Wang, and M. Rong, "High-Current Vacuum Arc: The Relationship Between Anode Phenomena and the Average Opening Velocity of Vacuum Interrupters," *IEEE Trans. Plasma Sci.*, vol. 39, pp. 1370-1378, Jun. 2011.

E-mail of the author(s): liuzy@mail.xjtu.edu.cn
kgw.fb@stu.xjtu.edu.cn